Spectral-Efficient Bidirectional Decode-and-Forward Relaying for Full-Duplex Communication

Li Li, Chen Dong, Li Wang, *Member, IEEE*, and Lajos Hanzo, *Fellow, IEEE*

***Abstract*—As a benefit of sophisticated interference cancelation techniques, full-duplex (FD) transceiver design may become feasible, even possibly on the aggressive time-scale of fifth-generation (5G) wireless communication systems. Hence, we further develop the recent bidirectional relaying [i.e., the two-way half-duplex (HD) relaying] aided cooperative network to its more radical counterpart, which entirely consists of FD entities for the sake of adapting to emerging FD communication scenarios. In more detail, the proposed bidirectional relaying-aided FD network operates in a decode-and-forward (DF) style and exploits the advanced network coding (NC) concept. We analyze its achievable error-free data rate, where the effects of both the self-interference (SI) and of the geographic location of the relay node (RN) are evaluated. Furthermore, the potential variations of the networking scenario are also taken into account. Based on this theoretical analysis, the optimum rate allocation scheme maximizing the system's error-free data rate is found. Our results demonstrate that a significant spectral efficiency gain is achieved by the proposed system.**

***Index Terms*—Author, please supply index terms/keywords for your paper. To download the IEEE Taxonomy go to http://www.ieee.org/documents/taxonomy_v101.pdf.**

I. Introduction

A set of cooperating mobiles may be viewed as a distributed multiple-input–multiple-output (MIMO) system relying on the spatially distributed single antennas of the cooperating mobiles, where the correlation of the antenna elements imposed by their insufficient separation experienced in conventional MIMO systems is efficiently avoided [1]. Furthermore, the detrimental path-loss effects may also be significantly mitigated by incorporating relay nodes (RNs) along the source-to-destination link, which results in an increased radio coverage area. However, despite these benefits, cooperation techniques impose their own problems as well. In the early stage of the node-cooperation research, constrained by the fact that practical transceivers cannot transmit and receive at the same time, the classic relaying regimes [2]–[4] had to rely on a pair of orthogonal channels for the reception and transmission at the RN. This implies that the conventional relaying regimes typically impose a factor-two throughput loss compared to their direct-transmission-based counterparts.

For the sake of recovering the throughput loss imposed by half-duplex (HD) relaying, sophisticated relaying protocols may be used [5]–[7]. For the particular scenario of two nodes exchanging messages with the aid of an RN, HD-based two-way relaying was devised in [5] and [8], which is capable of efficiently compressing the four distinct transmission phases required by conventional relaying regimes into three or even just two phases. Another conceptually straightforward solution conceived for avoiding the HD-relaying-induced throughput loss is that of replacing the HD relay (HDR) by a full-duplex relay (FDR). In this spirit, the early discussion of a practical FDR system was raised in [9]. The critical problem incurred in FDR is that a high-power interfering signal will be fed back to the RN's input from the RN's output, which results in the so-called "self-interference" (SI). Hence, abundant studies of the FDR concept focused on canceling or suppressing the SI, e.g., as shown in [10] and [11]. Along with the development of SI cancelation techniques, the theoretical analysis of the achievable performance of FDR systems was also carried out in [12]–[14], where the impact of SI was taken into account. Furthermore, the research of FDR systems was extended to multihop scenarios [15], [16].

However, if we extend our horizon a little further, the full-duplex (FD) transceiver design has substantial benefits beyond the scope of FDR systems. Recently, researchers at Stanford University made substantial progress in building FD radios [17], [18], although they still relied on utilizing multiple antennas. As a radical improvement of their early works, the first complete WiFi single-antenna aided FD link was reported a little later in [19], which is capable of reducing the SI to the noise floor by providing as much as 110 dB of linear cancelation, 80 dB of nonlinear cancelation, and 60 dB of analog cancelation. Based on these achievements in FD transceiver design, it is reasonable to expect that practical in-band FD systems may become a commercial reality in time for the emerging fifth-generation (5G) wireless networks [20].

Manuscript received April 20, 2015; revised August 6, 2015; accepted September 19, 2015. This work was supported by the National Natural Science Foundation of China (NSFC) under Project 61501383, by the National High-Tech R&D Program of China (863 Program) under Grant 2014AA01A707, by the Fundamental Research Funds for the Central Universities under Grant 2682015CX064, by the European Union under the auspices of the Concerto Project, by the Research Councils UK under the auspices of the India-UK Advanced Technology Centre known as IU-ATC, by European Research Council's Advanced Fellow Grant, and by the U.S. National Science Foundation under Grant CNS-1456793 and Grant ECCS-1343210. The review of this paper was coordinated by Dr. C. Xing.

L. Li is with the Provincial Key Laboratory of Information Coding and Transmission, Southwest Jiaotong University, Chengdu 610031, China, and also with the School of Electronics and Computer Science, University of Southampton Southampton SO17 1BJ, U.K. (e-mail: ll5e08@home.swjtu.edu.cn).

C. Dong is with the R&D Center of Huawei Technologies, Shenzhen 518129, China.

L. Wang is with the R&D Center of Huawei Technologies, 164 94 Stockholm, Sweden.

L. Hanzo is with the School of Electronics and Computer Science, University of Southampton, Southampton SO17 1BJ, U.K. (e-mail: lh@ecs.soton.ac.uk).

Digital Object Identifier 10.1109/TVT.2015.2483541

Given the aforementioned advances, the time has come for incorporating the FD technique into each and every component of a cooperative network. In this spirit, the early attempt of adapting the spectral-efficient two-way relaying protocol to an FD communication scenario had been reported by Cheng *et al.* [21] and by Cui *et al.* [22], where amplify-and-forward (AF) relaying and the associated analog network coding (NC) concept were invoked at the RN. Then, Zheng [23] further extended their networking prototype to a multihop architecture.

Against this background, our novel contributions are as follows:

- We conceive a network topology, where a pair of FD users exchange their information with the aid of an FD RN. Correspondingly, we propose the bidirectional decode-and-forward (DF) relaying concept for the sake of retaining the high spectral efficiency of FD communication, while reducing the path-loss effect. Based on DF relaying, a beneficial digital NC is conceived for the RN.
- We analyze the maximum achievable error-free data rate (MAEFDR) of the proposed bidirectional DF-relaying-aided FD network (BD-DF-FDN), where the effects of both the SI and of the geographic location of the RN are evaluated.
- The potential unbalance between the receive duration and the transmit duration of the RN is also taken into account in our analysis. Moreover, the MAEFDR of the proposed system is maximized by our optimum transmission rate allocation approach.

The remainder of this paper is organized as follows: The network topology of our bidirectional DF relaying regime and a range of important assumptions are introduced in Section II. Consecutively, the convex region of our system is characterized in Section III. Then, we commence the analysis of MAEFDR of the proposed BD-DF-FDN in Section IV, where the impact of the SI and that of the geographic RN location, as well as that of the variations of the network framework, are taken into account. Based on our optimum transmission rate allocation scheme, the simulation results characterizing the MAEFDR are provided in Section V. Finally, we conclude this paper in Section VI.

II. System Model

Here, we conceive the aforementioned bidirectional DF-relaying-aided FD network, which is referred to as "BD-DF-FDN," where two FD users, namely, "User 1" and "User 2," exchange their information with the aid of an FD-DF two-way (FD-DF-TW) RN. Observe in Fig. 1 that User 1 and User 2 broadcast their kth information frames $\mathbf{I}_1[k]$ and $\mathbf{I}_2[k]$ at the rates of R_1 and R_2, respectively. Correspondingly, the RN receives these signals and attempts to detect both $\mathbf{I}_1[k]$ and $\mathbf{I}_2[k]$ and then employs the advanced NC concept in [24]–[27] for creating another information frame $\mathbf{I}_3[k]$, which accommodates both the information carried by $\mathbf{I}_1[k]$ and that carried by $\mathbf{I}_2[k]$. In more detail, let $|\mathbf{I}[k]|$ represent the number of information bits carried by $\mathbf{I}[k]$. Then, without loss of generality, we may

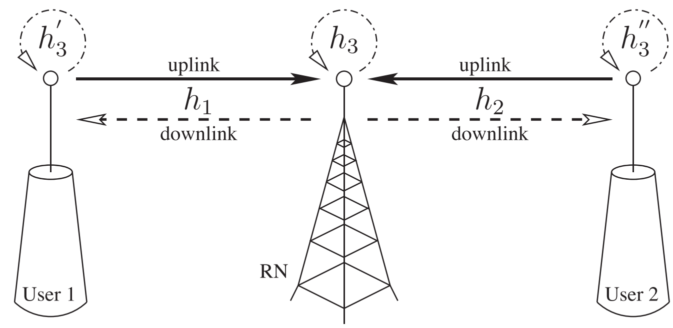

Fig. 1. Fundamental network topology of BD-DF-FDN: two FD users, namely, "User 1" and "User 2", exchange their information with the aid of an FD-DF-TW relaying-based RN.

assume that $|\mathbf{I}_2[k]| \geq |\mathbf{I}_1[k]|$.[1] Hence, after detecting $\mathbf{I}_1[k]$ and $\mathbf{I}_2[k]$, the RN pads the frame $\mathbf{I}_1[k]$ with zero bits for generating $\mathbf{I}_1^p[k]$, which satisfies $|\mathbf{I}_1^p[k]| = |\mathbf{I}_2[k]|$. Resultantly, the information frame $\mathbf{I}_3[k]$ is created by the XOR operation at the RN as follows:

$$\mathbf{I}_3[k] = \mathbf{I}_1^p[k] \oplus \mathbf{I}_2[k]. \tag{1}$$

The entire process described earlier may be referred to as the uplink (UL) of BD-DF-FDN.

As a substantial advantage of FD transceivers, along with the aforementioned UL transmission of BD-DF-FDN, the RN is capable of simultaneously forwarding the information frame $\mathbf{I}_3[k-\tau]$ in the same frequency band to both User 1 and to User 2, which was generated by the RN τ time slots ago. Meanwhile, User 1 attempts to detect $\mathbf{I}_2[k-\tau]$, namely, the frame that was originally transmitted by User 2 and carried by $\mathbf{I}_3[k-\tau]$, which is achieved by implementing the XOR operation of $\mathbf{I}_1^p[k-\tau] \oplus \mathbf{I}_3[k-\tau]$. A similar detection process is implemented by User 2. These operations constitute the downlink (DL) of the BD-DF-FDN in Fig. 1.

As shown at the top of the antennas of User 1 and of User 2 as well as of the RN in Fig. 1, the high-power transmitted signal of these transceivers will be fed back to their receiver's input, which results in the SI problem. Hence, instead of directly forwarding $\mathbf{I}_3[k]$, the RN forwards a previously generated information frame $\mathbf{I}_3[k-\tau]$ in the DL of BD-DF-FDN, for the sake of guaranteeing that the output of the RN always remains uncorrelated with its simultaneous input, which is a precondition of achieving high-quality SI cancelation, as detailed in [11] and [13]. The number of information bits transmitted by the RN has to be equal to that input into it. Hence, $\mathbf{I}_3[k-\tau]$ and $\mathbf{I}_3[k]$ have the same number of information bits.[2] Moreover, it is assumed that User 1, User 2, and the RN may have the same SI suppression capability, owing to employing the same FD transceiver technique.

Definition 2.1: The time required by User 1 and 2 for transmitting $\mathbf{I}_1[k]$ and $\mathbf{I}_2[k]$ to the RN via the UL of the BD-DF-FDN

[1]Without loss of generality, we explicitly take the case of $|\mathbf{I}_2[k]| >= |\mathbf{I}_1[k]|$ as an example. Apparently, the detailed NC operations associated with another case of $|\mathbf{I}_2[k]| < |\mathbf{I}_1[k]|$ should obey similar principles.

[2]This implies that if $\mathbf{I}_3[k-\tau] = \mathbf{I}_1^p[k-\tau] \oplus \mathbf{I}_2[k-\tau]$, then we may assume that $|\mathbf{I}_3[k-\tau]| = |\mathbf{I}_3[k]|$, $|\mathbf{I}_1^p[k-\tau]| = |\mathbf{I}_1^p[k]|$, and $|\mathbf{I}_2[k-\tau]| = |\mathbf{I}_2[k]|$.

in Fig. 1 is regarded as the UL period. Simultaneously, the time required by the RN for broadcasting $\mathbf{I}_3[k]$ to both User 1 and 2 via the DL of the BD-DF-FDN is regarded as the DL period. Finally, the time required for completing a pair of UL and DL periods is regarded as a complete BD-DF-FDN period. Naturally, the BD-DF-FDN period is equal to max [UL period, DL period].

The path-loss reduction gain (PLRG) achieved by the reduced transmission distance experienced in cooperative systems is introduced next. As detailed in [28], the average PLRGs of the User-1-to-RN link and of the User-2-to-RN link are given by $G_1 = (D/D_1)^{\alpha}$ and $G_2 = (D/D_2)^{\alpha}$, respectively, where D, D_1, D_2 are the distances from User 1 to User 2, from User 1 to the RN, and from User 2 to the RN, respectively. Throughout this paper, the path-loss exponent is fixed to $\alpha = 4$, for representing a typical urban area. In practice, the direct link between User 1 and User 2 of our system may become weak, while simultaneously being interfered by the strong contaminating signal of the RN. Hence, similar to [21] and [22], it may be reasonable to ignore the signal received via this direct link in Fig. 1. Then, all the possible propagation paths in our BD-DF-FDN are assumed to be the flat block-fading Rayleigh channels, where the fading coefficient of a channel remains constant over a block period but fluctuates in a flat independent Rayleigh fading manner among different blocks. It is also assumed that they are reciprocal channels, which means that the channel from User 1 to the RN is identical to that from the RN to User 1 during the same period. Furthermore, we assumed that a BD-DF-FDN period happens to overlap a block period of the associated channels. Finally, we do not consider any sophisticated power allocation scheme in this paper. We equitably share the entire power among User 1, User 2, and the RN, i.e., we have $P_1 = P_2 = P_3 = P$, where P_1, P_2, P_3 is the transmit power of User 1, User 2, and the RN, respectively.

Based on these assumptions, the signal received at the RN within the transmission of a specific information frame is given by $y_3 = h_1\sqrt{G_1}S_1 + h_2\sqrt{G_2}S_2 + h_3S_3 + n_3$, where h_1 and h_2 are the fading coefficients of the User-1-to-RN link and of the User-2-to-RN link, respectively, while S_1, S_2, S_3 represent the symbols transmitted by User 1, User 2, and the RN, respectively. Finally, n_3 is the additive white Gaussian noise (AWGN) imposed on the RN, which obeys $n_3 \sim \mathcal{CN}(0, \sigma^2)$. Specifically, the signal component h_3S_3 captures the SI imposed on the RN, as shown in Fig. 1, where h_3 may be regarded as the attenuation of the SI channel. After implementing the SI cancelation, the residual SI becomes $\tilde{h}_3S_3$, owing to a potentially imperfect cancelation process. Let us define the SI suppression factor as $G_{\rm SI} = 1/|\tilde{h}_3|^2$, which is inversely proportional to the power of the residual SI. Consequently, after SI cancelation, the received signal y_3 may be modified to

$$y_3 = h_1\sqrt{G_1}S_1 + h_2\sqrt{G_2}S_2 + \tilde{h}_3S_3 + n_3. \tag{2}$$

III. Convex Region of $(R_1 + R_2)$

Based on the system model built in Section II, particularly on the physical concepts introduced in Section II, we now define the relevant SNRs as follows:

$$\gamma_1 = \frac{|h_1|^2 G_1 P_1}{\sigma^2}, \quad \gamma_2 = \frac{|h_2|^2 G_2 P_2}{\sigma^2}$$
$$\gamma_3 = \frac{|\tilde{h}_3|^2 P_3}{\sigma^2} = \frac{P_3}{\sigma^2 \cdot G_{\rm SI}}. \tag{3}$$

Without loss of generality, we may assume that[3] $\gamma_2 \geq \gamma_1$.

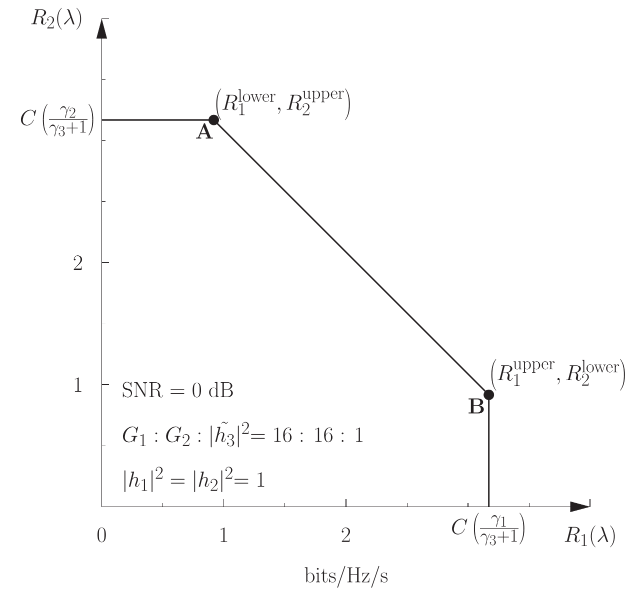

Fig. 2. Convex region of the rate pair $(R_1 + R_2)$, where a scenario having "SNR = 0 dB; $G_1 : G_2 : |\tilde{h}_3|^2 = 16 : 16 : 1$; $|h_1|^2 = |h_2|^2 = 1$" is considered as an example.

Since the RN in Fig. 1 relies on the DF protocol, we have to carefully avoid the error propagation problem. Hence, the transmission rates R_1 and R_2 have to be specifically chosen to ensure that the information frames $\mathbf{I}_1[k]$ and $\mathbf{I}_2[k]$ can be perfectly decoded at the RN. According to the multiple-access channel capacity theorem in [29], these rate pairs (R_1, R_2) have to lie within the convex region shown in Fig. 2. Furthermore, the rate pairs (R_1, R_2) distributed along the segment $\overline{\mathbf{AB}}$ will result in the maximum sum rate of $(R_1 + R_2)$.

In more detail, considering the UL in Fig. 1, if the RN first decodes the information frame $\mathbf{I}_1[k]$, it may regard the information frame $\mathbf{I}_2[k]$ as a contamination. Hence, according to (2), the overall signal-to-inference-plus-noise power ratio (SINR) of the User-1-to-RN link is given by

$$\begin{aligned}\mathrm{SINR}_{1\to 3} &= \frac{|h_1|^2 G_1 P_1}{|h_2|^2 G_2 P_2 + |\tilde{h}_3|^2 P_3 + \sigma^2} \\ &= \frac{\gamma_1}{\gamma_2 + \gamma_3 + 1}.\end{aligned} \tag{4}$$

In this case, the associated capacity of the User-1-to-RN link may be formulated as[4] $C(\gamma_1/(\gamma_2 + \gamma_3 + 1))$, which is also the lower bound of R_1, namely, $R_1^{\rm lower}$, when simultaneously satisfying the flawless decodability of information frames received at the RN, while simultaneously attaining the maximum sum rate of $(R_1 + R_2)$.

[3] This implies that the higher one between γ_1 and γ_2 is always represented by the label "γ_2."

[4] It is exploited herein that $C(x) = \log_2(1 + x)$.

Then, the RN proceeds to decode the information frame $I_2[k]$. Since the information frame $I_1[k]$ has been perfectly decoded, the RN is capable of perfectly eliminating the interference component $h_1\sqrt{G_1}S_1$ from (2).[5] Resultantly, the SINR of the User-2-to-RN link is given by

$$\mathrm{SINR}_{2\to 3} = \frac{|h_2|^2 G_2 P_2}{|\tilde{h}_3|^2 P_3 + \sigma^2} = \frac{\gamma_2}{\gamma_3 + 1}$$

which yields the upper bound of R_2, namely, R_2^{upper}. Hence, we obtain a specific rate pair of $(R_1 + R_2)$ as follows:

$$\begin{cases} R_1^{\mathrm{lower}} = C\left(\frac{\gamma_1}{\gamma_2+\gamma_3+1}\right) \\ R_2^{\mathrm{upper}} = C\left(\frac{\gamma_2}{\gamma_3+1}\right) \end{cases} \quad (5)$$

which corresponds to the point $\mathbf{A}(R_1^{\mathrm{lower}}, R_2^{\mathrm{upper}})$ in Fig. 2, and it is referred to as Case $\mathbf{A}$.

Alternatively, the RN may first decode $\mathbf{I}_2[k]$ and then proceed to decode $\mathbf{I}_1[k]$. Correspondingly, this case results in the lower bound of R_2 and the upper bound of R_1, which may be formulated as Case $\mathbf{B}$ as follows:

$$\begin{cases} R_1^{\mathrm{upper}} = C\left(\frac{\gamma_1}{\gamma_3+1}\right) \\ R_2^{\mathrm{lower}} = C\left(\frac{\gamma_2}{\gamma_1+\gamma_3+1}\right). \end{cases} \quad (6)$$

This is represented as the point $\mathbf{B}(R_1^{\mathrm{upper}}, R_2^{\mathrm{lower}})$ in Fig. 2.

Apparently, the UL of our BD-DF-FDN shown in Fig. 1 operates in either the aforementioned Case $\mathbf{A}$ or Case $\mathbf{B}$. Hence, we may proceed by invoking the time-sharing parameter [8] (or rate-allocation parameter) of "$\lambda, 0 \le \lambda \le 1$," for characterizing the ratio of the time operating in Case $\mathbf{A}$ to the time operating in Case $\mathbf{B}$. If the fraction of time operating in Case $\mathbf{B}$ is λ, then according to (5) and (6), the average transmission rates of User 1 and User 2 may be formulated as $R_1(\lambda) = \lambda R_1^{\mathrm{upper}} + (1-\lambda)R_1^{\mathrm{lower}}$ and $R_2(\lambda) = \lambda R_2^{\mathrm{lower}} + (1-\lambda)R_2^{\mathrm{upper}}$, respectively. Hence, we arrive at Theorem 3.1.

Theorem 3.1: To simultaneously satisfy both the decodability of the information frames received at the RN and the attainability of the maximum sum rate of the BD-DF-FDN shown in Fig. 1, the rate pairs $[R_1(\lambda), R_2(\lambda)]$ have to obey

$$\begin{cases} R_1(\lambda) = \lambda\left[C\left(\frac{\gamma_1}{\gamma_3+1}\right) - C\left(\frac{\gamma_1}{\gamma_2+\gamma_3+1}\right)\right] \\ \qquad + C\left(\frac{\gamma_1}{\gamma_2+\gamma_3+1}\right), \quad 0 \le \lambda \le 1 \\ R_2(\lambda) = \lambda\left[C\left(\frac{\gamma_2}{\gamma_1+\gamma_3+1}\right) - C\left(\frac{\gamma_2}{\gamma_3+1}\right)\right] \\ \qquad + C\left(\frac{\gamma_2}{\gamma_3+1}\right), \quad 0 \le \lambda \le 1 \end{cases} \quad (7)$$

where $R_1(\lambda)$ or $R_2(\lambda)$ is the transmit rate of User 1 or User 2 during the UL period, respectively. λ is the time-sharing parameter, which determines the time that User i transmits in its upper bound rate R_i^{upper} and in its lower bound rate R_i^{lower}. The rate pairs of $[R_1(\lambda), R_2(\lambda)]$ stipulated by (7) constitute the segment $\overline{\mathbf{AB}}$ in Fig. 2.

[5]In this paper, we assume that perfect channel-state information (CSI) is always available at the receivers. Moreover, since all the nodes of BD-DF-FDN work in FD style and the related channels are assumed to be reciprocal, this assumption will also result in CSI becoming available at the transmitters.

IV. Maximum Achieveable Error-Free Data Rate

Based on the fundamental architecture of BD-DF-FDN, as demonstrated in Fig. 1 in Section II, we will categorize the BD-DF-FDN into several distinct scenarios. In different subcases, its MAEFDR will be characterized by different formulas. During the entire derivation process, the rate pair of $(R_1(\lambda), R_2(\lambda))$ will obey the convex region stipulated in Section III. Particularly, the monotonicity determined by (7) will be referred to frequently.

A. *Case 1:* $\gamma_2 \ge \gamma_1 + (1/(\gamma_3+1))\gamma_1^2$

In this case, we have the relationship of $C(\gamma_2/(\gamma_1+\gamma_3+1)) \ge C(\gamma_1/(\gamma_3+1))$. According to (7), $R_2(\lambda)$ is a monotonically decreasing function of the rate-allocation parameter λ, while $R_1(\lambda)$ is a monotonically increasing function of λ, and $R_2(1) = C(\gamma_2/(\gamma_1+\gamma_3+1))$, $R_1(1) = C(\gamma_1/(\gamma_3+1))$. Hence, we can readily arrive at

$$R_2(\lambda) \ge C\left(\frac{\gamma_2}{\gamma_1+\gamma_3+1}\right) \ge C\left(\frac{\gamma_1}{\gamma_3+1}\right) \ge R_1(\lambda). \quad (8)$$

Then, observe in the DL in Fig. 1 that similar to the derivation of (4) and (5), the SINR of the RN-to-User-1 link is given by $\mathrm{SINR}_{3\to 1} = |h_1|^2 G_1 P_3/(|\tilde{h}_3'|^2 P_1 + \sigma^2)$. Since we assumed in Section II that User 1, User 2, and the RN have the same SI suppression capability, it is reasonable to assume that $|\tilde{h}_3'|^2 = |\tilde{h}_3|^2$. Then, as stated in Section II, we have $P_1 = P_2 = P_3$. Hence, we may arrive at

$$\mathrm{SINR}_{3\to 1} = \frac{\gamma_1}{\gamma_3 + 1}. \quad (9)$$

Therefore, the capacity of the RN-to-User-1 link is $C(\gamma_1/(\gamma_3+1))$. Similarly, it can be shown that the capacity of the RN-to-User-2 link is $C(\gamma_2/(\gamma_3+1))$.

To satisfy that $\mathbf{I}_2[k]$ and $\mathbf{I}_1[k]$ are decodable by User 1 and 2, respectively, $\mathbf{I}_3[k]$ has to be transmitted at the lower rate between the capacity of the RN-to-User-1 link and that of the RN-to-User-2 link. Since we have $C(\gamma_2/(\gamma_3+1)) \ge C(\gamma_1/(\gamma_3+1))$, $\mathbf{I}_3[k]$ is first transmitted at the rate of $C(\gamma_1/(\gamma_3+1))$. As stated in Section II, the amount of information transmitted via the User-2-to-RN link during the UL period is identical to that transmitted via the RN-to-User-1 link during the DL period. However, according to (8), we have $R_2(\lambda) \ge C(\gamma_1/(\gamma_3+1))$. Hence, it can be anticipated that the UL transmission session shown in Fig. 1 will terminate earlier than the DL session. Consequently, the framework of the BD-DF-FDN shown in Fig. 1 is actually transformed into that shown in Fig. 3, where the time following the termination of the UL period up to the completion of the DL transmission is referred to as the "Residual-Period."

As illustrated in Fig. 3, transmitting $\mathbf{I}_1[k]$ and $\mathbf{I}_2[k]$ to the RN is completed during the UL period at the rates of $R_1(\lambda)$ and $R_2(\lambda)$, respectively, which implies that we may have $|\mathbf{I}_1[k]| = NR_1(\lambda)$, $|\mathbf{I}_2[k]| = NR_2(\lambda)$, where N is the time required for transmitting $|\mathbf{I}_1[k]|$ number of information bits at the rate of $R_1(\lambda)$.[6]

[6]Alternatively, N is also the time required for transmitting $|\mathbf{I}_2[k]|$ information bits at the rate of $R_2(\lambda)$.

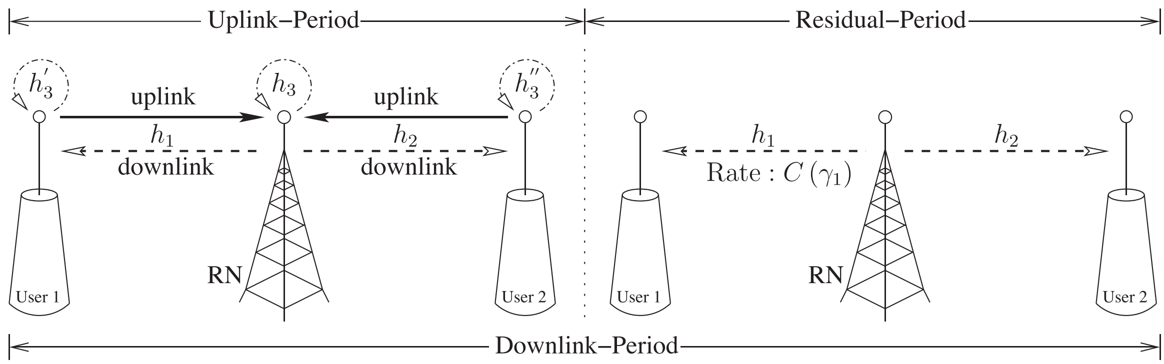

Fig. 3. Practical framework of the BD-DF-FDN in the case of $\gamma_2 \geq \gamma_1 + (1/(\gamma_3+1))\gamma_1^2$.

As stated before, during the DL period, the RN will first broadcast $\mathbf{I}_3[k]$ at the lower rate between the capacity of the RN-to-User-1 link and that of the RN-to-User-2 link, until the specific one from the set of $\mathbf{I}_1[k]$ and $\mathbf{I}_2[k]$, which carries less information bits, has been completely transmitted/received. In this case, according to (8), we have $R_2(\lambda) \geq R_1(\lambda)$, which leads to $|\mathbf{I}_2[k]| \geq |\mathbf{I}_1[k]|$. Hence, the transmission of the information bits of $\mathbf{I}_1[k]$ via the RN-to-User-2 link will terminate first during the DL period. Accordingly, the length of the residual period shown in Fig. 3 is determined by the transmission of the information bits of $\mathbf{I}_2[k]$ via the RN-to-User-1 link.

During the UL period, the RN broadcasts $\mathbf{I}_3[k]$ at the rate of $C(\gamma_1/(\gamma_3+1))$. Hence, during the residual period, there are $[|\mathbf{I}_2[k]| - N \cdot C(\gamma_1/(\gamma_3+1))]$ information bits of $\mathbf{I}_2[k]$, which still have to be transmitted via the RN-to-User-1 link. Meanwhile, since the transmission via the UL has been terminated, we would no longer incur any SI during the residual period. Consequently, the capacity of the RN-to-User-1 link is increased to $C(\gamma_1)$. Hence, the length of the residual period should be $(|\mathbf{I}_2[k]| - NC(\gamma_1/(\gamma_3+1)))/C(\gamma_1)$.

Definition 4.1: We divide the number of decodable information bits exchanged between User 1 and User 2 with the aid of our BD-DF-FDN by the associated time to define the overall achievable error-free data rate.

Hence, the achievable error-free data rate of BD-DF-FDN for Case 1 is given by

$$\begin{aligned} &R^{\text{BD-DF-FDN, Case 1}}(\lambda) \\ &= \frac{|\mathbf{I}_1[k]| + |\mathbf{I}_2[k]|}{\text{BD-DF-FDN period}} \\ &= \frac{NR_1(\lambda) + NR_2(\lambda)}{N + \frac{|\mathbf{I}_2[k]| - NC\left(\frac{\gamma_1}{\gamma_3+1}\right)}{C(\gamma_1)}} \\ &= \frac{C\left(\frac{\gamma_1+\gamma_2}{\gamma_3+1}\right) C(\gamma_1)}{C(\gamma_1) - C\left(\frac{\gamma_1}{\gamma_3+1}\right) + R_2(\lambda)}. \end{aligned} \tag{10}$$

According to (10), $R^{\text{BD-DF-FDN, Case 1}}(\lambda)$ is a monotonically decreasing function of $R_2(\lambda)$. Hence, we may assign to User 2 its minimum transmission rate of $R_2(1) = C(\gamma_2/(\gamma_1 + \gamma_3 + 1))$ during the UL period of BD-DF-FDN. Given this optimum rate allocation scheme, the MAEFDR of Case 1 of BD-DF-FDN may be expressed as

$$R_{\max}^{\text{BD-DF-FDN}} = \frac{C\left(\frac{\gamma_1+\gamma_2}{\gamma_3+1}\right) C(\gamma_1)}{C(\gamma_1) + C\left(\frac{\gamma_2}{\gamma_1+\gamma_3+1}\right) - C\left(\frac{\gamma_1}{\gamma_3+1}\right)} \quad \text{if } \gamma_2 \geq \gamma_1 + \left(\frac{1}{\gamma_3+1}\right)\gamma_1^2. \tag{11}$$

B. *Case 2:* $\gamma_1 + (1/(\gamma_3+1))\gamma_1^2 > \gamma_2 \geq \gamma_1$

In this case, it is possible to arrive at

$$\begin{cases} R_2(\lambda_1) = C\left(\frac{\gamma_1}{\gamma_3+1}\right) \\ R_2(\lambda_0) = R_1(\lambda_0) \end{cases} \tag{12}$$

where the specific values of the associated rate-allocation parameters are given by

$$\begin{cases} \lambda_1 = \frac{C\left(\frac{\gamma_2}{\gamma_3+1}\right) - C\left(\frac{\gamma_1}{\gamma_3+1}\right)}{C\left(\frac{\gamma_1}{\gamma_3+1}\right) + C\left(\frac{\gamma_2}{\gamma_3+1}\right) - C\left(\frac{\gamma_1+\gamma_2}{\gamma_3+1}\right)} \\ \lambda_0 = \frac{C\left(\frac{\gamma_2}{\gamma_3+1}\right) - \frac{1}{2}C\left(\frac{\gamma_1+\gamma_2}{\gamma_3+1}\right)}{C\left(\frac{\gamma_1}{\gamma_3+1}\right) + C\left(\frac{\gamma_2}{\gamma_3+1}\right) - C\left(\frac{\gamma_1+\gamma_2}{\gamma_3+1}\right)}. \end{cases} \tag{13}$$

Based on (13) as well as on the condition of $\gamma_1 + (1/(\gamma_3+1))\gamma_1^2 > \gamma_2 \geq \gamma_1$, it can be shown that

$$0 \leq \lambda_1 < \lambda_0 < 1. \tag{14}$$

Hence, as our next step, we further divide "Case 2" into several subclasses according to the range of λ.

1) Case 2.1, Where $\lambda \in [0, \lambda_1]$: According to (7), $R_2(\lambda)$ is a monotonically decreasing function of λ. Since $\lambda \leq \lambda_1$, we have $R_2(\lambda) \geq R_2(\lambda_1)$. Then, $R_1(\lambda)$ is a monotonically increasing function of λ. Since $1 > \lambda$, we arrive at $R_1(1) > R_1(\lambda)$. According to (12), we have $R_2(\lambda_1) = C(\gamma_1/(\gamma_3+1)) = R_1(1)$. Finally, we arrive at $R_2(\lambda) \geq C(\gamma_1/(\gamma_3+1)) > R_1(\lambda)$, which is almost the same as the relationship given in (8). This implies that the achievable error-free data rate for Case 2.1 of BD-DF-FDN may be characterized by the same formula as that given in (10). The only difference is that, in Case 1, the minimum transmission rate, which can be assigned to User 2, is $C(\gamma_2/(\gamma_1+\gamma_3+1))$. By contrast, in Case 2.1, this becomes $C(\gamma_1/(\gamma_3+1))$, owing to the rate-allocation strategy specified according to $\lambda \in [0, \lambda_1]$. Resultantly, after substituting the new

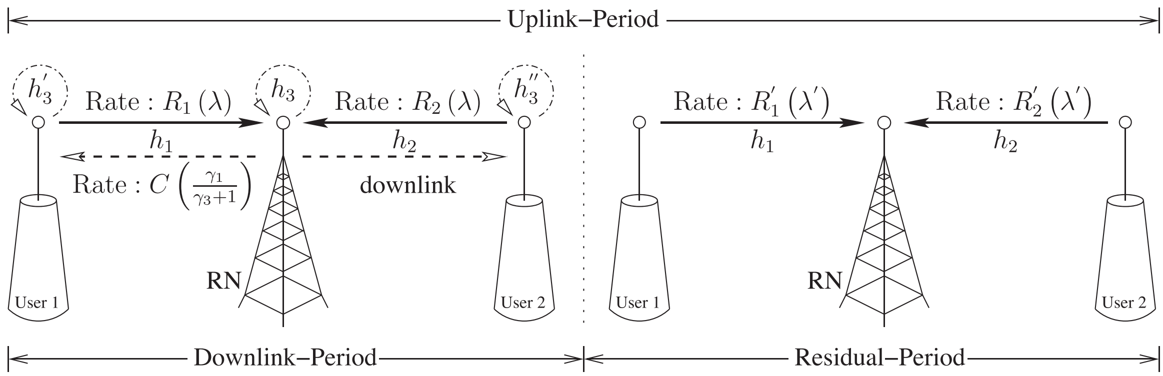

Fig. 4. Practical framework of the BD-DF-FDN in Fig. 1 in the case of $\gamma_1 + (1/(\gamma_3+1))\gamma_1^2 > \gamma_2 \geq \gamma_1 \cap \lambda \in (\lambda_1, \lambda_0]$.

minimum transmission rate of User 2, i.e., $C(\gamma_1/(\gamma_3+1))$, into (10), we arrive at the MAEFDR for Case 2.1 of BD-DF-FDN, which is given by

$$R_{\max}^{\mathrm{BD-DF-FDN}} = C\left(\frac{\gamma_1+\gamma_2}{\gamma_3+1}\right) \quad \text{if } \gamma_1 + \left(\frac{1}{\gamma_3+1}\right)\gamma_1^2 > \gamma_2 \geq \gamma_1 \cap \lambda \in [0, \lambda_1] \tag{15}$$

where the UL and DL transmissions of BD-DF-FDN happen to be completed simultaneously.

2) Case 2.2, Where $\lambda \in (\lambda_1, \lambda_0]$: We commence by stating that the number of information bits transmitted by User 1 and User 2 during the UL period have a ratio of

$$\frac{|\mathbf{I}_2[k]|}{|\mathbf{I}_1[k]|} = \frac{R_2(\lambda)}{R_1(\lambda)}, \quad \lambda \in (\lambda_1 \lambda_0] \tag{16}$$

which is supposed to be the optimum allocation of the number AQ4 of information bits $|\mathbf{I}_2[k]|, |\mathbf{I}_2[k]|$ in terms of maximizing the overall achievable error-free data rate of Case 2.2.

Again, since $R_2(\lambda)$ is a monotonically decreasing function of λ and $\lambda_1 < \lambda \leq \lambda_0$, we can readily arrive at the conclusion that $R_2(\lambda_1) > R_2(\lambda) \geq R_2(\lambda_0)$. Then, because $R_1(\lambda)$ is a monotonically increasing function of λ, we conclude that $R_1(\lambda_0) \geq R_1(\lambda)$. By recalling from (12) that $R_2(\lambda_1) = C(\gamma_1/(\gamma_3+1))$, $R_2(\lambda_0) = R_1(\lambda_0)$, it can be readily shown for Case 2.2 that

$$C\left(\frac{\gamma_1}{\gamma_3+1}\right) > R_2(\lambda) \geq R_1(\lambda). \tag{17}$$

According to (16) and (17), we get $|\mathbf{I}_2[k]| \geq |\mathbf{I}_1[k]|$. Hence, following the principles detailed in Section IV-A, in Case 2.2, the length of the DL period is determined by the transmission of the information bits of $\mathbf{I}_2[k]$ via the RN-to-User-1 link, since $\mathbf{I}_2[k]$ carries more information bits than $\mathbf{I}_1[k]$. Furthermore, before either the UL or the DL completes its transmission, the transmission of the information bits of $\mathbf{I}_2[k]$ via the RN-to-User-1 link is carried out at the same rate of $C(\gamma_1/(\gamma_3+1))$. Meanwhile, the transmission of the information bits of $\mathbf{I}_2[k]$ via the User-2-to-RN link, which determines the transmit duration of the UL, is carried out at the rate of $R_2(\lambda)$. Hence, according to (17), we get $C(\gamma_1/(\gamma_3+1)) > R_2(\lambda)$, which implies that, in Case 2.2, the DL transmission will terminate earlier than the UL transmission. Consequently, the framework of the BD-DF-FDN shown in Fig. 1 is actually transformed into that shown in Fig. 4 for Case 2.2. In this scenario, the definition of the "Residual-Period" has been changed to the time duration following the termination of the DL period and spanning to the end of the UL transmission.

Observe in Fig. 4 that, according to the aforementioned analysis, the length of the entire DL period is determined by the transmission of the information bits of $\mathbf{I}_2[k]$ via the RN-to-User-1 link at the fixed rate of $C(\gamma_1/(\gamma_3+1))$, which is given by $T = |\mathbf{I}_2[k]|/C(\gamma_1/(\gamma_3+1)) = NR_2(\lambda)/C(\gamma_1/(\gamma_3+1))$, where N is still defined as the time required for transmitting $|\mathbf{I}_2[k]|$ number of information bits at the rate of $R_2(\lambda)$. Resultantly, the number of residual information bits of $\mathbf{I}_1[k]$ and $\mathbf{I}_2[k]$, which pertain to the UL transmission and will be transmitted during the ensuing residual period, are given by $(|\mathbf{I}_1[k]| - TR_1(\lambda))$ and $(|\mathbf{I}_2[k]| - TR_2(\lambda))$, respectively.

Observe during the residual period in Fig. 4 that, when the transmissions via the DL are terminated, the detrimental SI naturally disappears, which simplifies the architecture of our BD-DF-FDN to the first step of conventional two-way relaying, as shown for example in [8, Fig. 1(b)]. Therefore, the optimum transmission rate proposed in [8], which was detailed in [8, (25–28)], becomes applicable to the residual period in Fig. 4. Consequently, during the residual period in Fig. 4, according to [8, (25–28)], Theorem 3.1 is modified to

$$\begin{cases} R'_1(\lambda') = \lambda'\left[C(\gamma_1) - C\left(\frac{\gamma_1}{\gamma_2+1}\right)\right] \\ \qquad\qquad + C\left(\frac{\gamma_1}{\gamma_2+1}\right), \quad 0 \leq \lambda' \leq 1 \\ R'_2(\lambda') = \lambda'\left[C\left(\frac{\gamma_2}{\gamma_1+1}\right) - C(\gamma_2)\right] \\ \qquad\qquad + C(\gamma_2), \quad 0 \leq \lambda' \leq 1 \end{cases} \tag{18}$$

where the rate pairs $[R'_1(\lambda'), R'_2(\lambda')]$ are capable of maximizing the sum rate of the UL during the residual period in Fig. 4, which hence will be utilized for updating the transmission rates of User 1 and 2 during this period.

Additionally, the transmissions of the residual information bits of $\mathbf{I}_1[k]$ and $\mathbf{I}_1[k]$ at the rates of $R'_1(\lambda')$ and $R'_2(\lambda')$, respectively, should be completed simultaneously, which implies that AQ5 we have to find a rate pair of $[R'_1(\lambda'), R'_2(\lambda')]$, which satisfies

$$\frac{(|\mathbf{I}_1[k]| - TR_1(\lambda))}{R'_1(\lambda')} = \frac{(|\mathbf{I}_2[k]| - TR_2(\lambda))}{R'_2(\lambda')}. \tag{19}$$

The condition stipulated by (19) may be identically transformed to

$$\frac{R_2(\lambda)}{R_1(\lambda)} = \frac{R_2'(\lambda')}{R_1'(\lambda')}. \tag{20}$$

Then, it can be shown that, under the condition of $\gamma_1 + (1/(\gamma_3+1))\gamma_1^2 > \gamma_2 \geq \gamma_1$, we always have $R_2(\lambda)/R_1(\lambda) \in [1, (C(\gamma_1/(\gamma_3+1))/C(\gamma_2/(\gamma_1+\gamma_3+1)))$, $(R_2'(\lambda')/R_1'(\lambda')) \in [(C(\gamma_2/(\gamma_1+1))/C(\gamma_1)), (C(\gamma_2)/C(\gamma_1/(\gamma_2+1)))]$ and $[1, (C(\gamma_1/(\gamma_3+1))/C(\gamma_2/(\gamma_1+\gamma_3+1))) \subset [(C(\gamma_2/(\gamma_1+1))/C(\gamma_1)), (C(\gamma_2)/C(\gamma_1/(\gamma_2+1)))]$. Since the range of $R_2(\lambda)/R_1(\lambda)$ is always included within the range of $R_2'(\lambda')/R_1'(\lambda')$, there is always a solution of λ', which is capable of satisfying $R_2(\lambda)/R_1(\lambda) = R_2'(\lambda')/R_1'(\lambda')$, regardless of the value of $R_2(\lambda)/R_1(\lambda)$. This implies that the allocation of the number of information bits represented by (16), which inherently satisfies Theorem 3.1, will not conflict with the modified one in (18), hence allowing us to maximize the overall achievable error-free data rate of Case 2.2. AQ6

Based on the holistic analysis presented in Section IV-B2, the overall achievable error-free data rate of Case 2.2 is given by

$$\begin{aligned} &R^{\text{BD-DF-FDN, Case 2.2}}(\lambda) \\ &= \frac{|\mathbf{I}_1[k]| + |\mathbf{I}_2[k]|}{\text{DL-period} + \text{residual-period}} \\ &= \frac{NR_1(\lambda) + NR_2(\lambda)}{T + \frac{(|\mathbf{I}_1[k]| - TR_1(\lambda)) + (|\mathbf{I}_2[k]| - TR_2(\lambda))}{R_1'(\lambda') + R_2'(\lambda')}} \\ &= \frac{C(\gamma_1+\gamma_2) C\left(\frac{\gamma_1+\gamma_2}{\gamma_3+1}\right) C\left(\frac{\gamma_1}{\gamma_3+1}\right)}{C\left(\frac{\gamma_1+\gamma_2}{\gamma_3+1}\right) C\left(\frac{\gamma_1}{\gamma_3+1}\right) + R_2(\lambda)\left[C(\gamma_1+\gamma_2) - C\left(\frac{\gamma_1+\gamma_2}{\gamma_3+1}\right)\right]}. \end{aligned} \tag{21}$$

According to (21), $R^{\text{BD-DF-FDN, Case 2.2}}(\lambda)$ is a monotonically decreasing function of $R_2(\lambda)$. Hence, if we allocate its minimum transmission rate of $R_2(\lambda_0)$ to User 2 for the period preceding the residual period, we arrive at the MAEFDR of Case 2.2, which is formulated as

$$R_{\max}^{\text{BD-DF-FDN}} = \frac{C(\gamma_1+\gamma_2) C\left(\frac{\gamma_1}{\gamma_3+1}\right)}{C\left(\frac{\gamma_1}{\gamma_3+1}\right) + \frac{1}{2}\left[C(\gamma_1+\gamma_2) - C\left(\frac{\gamma_1+\gamma_2}{\gamma_3+1}\right)\right]}$$
$$\text{if } \gamma_1 + \left(\frac{1}{\gamma_3+1}\right)\gamma_1^2 > \gamma_2 \geq \gamma_1 \cap \lambda \in (\lambda_1, \lambda_0]. \tag{22}$$

3) Case 2.3, Where $\lambda \in (\lambda_0, 1]$*:* Similar to the assumption made at the beginning of Section IV-B2, the number of information bits $|\mathbf{I}_2[k]|$ and $|\mathbf{I}_1[k]|$ also have a ratio of

$$\frac{|\mathbf{I}_2[k]|}{|\mathbf{I}_1[k]|} = \frac{R_2(\lambda)}{R_1(\lambda)}, \quad \lambda \in (\lambda_0, 1] \tag{23}$$

which is supposed to be capable of maximizing the achievable error-free data rate of Case 2.3.

Again, according to the monotonicity of $R_1(\lambda)$ and $R_2(\lambda)$, as shown in (7), as well as by invoking (12), it can be shown for Case 2.3 that we have

$$C\left(\frac{\gamma_1}{\gamma_3+1}\right) \geq R_1(\lambda) > R_2(\lambda). \tag{24}$$

According to (23) and (24), it can be shown that $|\mathbf{I}_1[k]| > |\mathbf{I}_2[k]|$.

Observe in Fig. 1 that, during the DL transmission, again, $\mathbf{I}_2[k]$ number of information bits are transmitted via the RN-to-User-1 link at the rate of $C(\gamma_1/(\gamma_3+1))$. The associated time required for completing the transmission of the information bits of $\mathbf{I}_2[k]$ via the RN-to-User-1 link is given by

$$T_1 = \frac{|\mathbf{I}_2[k]|}{C\left(\frac{\gamma_1}{\gamma_3+1}\right)}. \tag{25}$$

Since we have $|\mathbf{I}_1[k]| > |\mathbf{I}_2[k]|$, after broadcasting $\mathbf{I}_3[k]$ at the rate of $C(\gamma_1/(\gamma_3+1))$ for a time duration of T_1, the RN has to continue with the transmission of the residual information bits of $\mathbf{I}_1[k]$ via the RN-to-User-2 link. According to the NC scheme employed at the RN, which was introduced in Section II, from now on, only the zero padding bits of $\mathbf{I}_2[k]$ are still being transmitted via the RN-to-User-1 link. Hence, we only have to consider the decodability of the transmission via the RN-to-User-2 link. Correspondingly, from now on, the RN will broadcast $\mathbf{I}_3[k]$ at a higher rate of $C((\gamma_2/(\gamma_3+1))$. The time required for completing the transmission of the residual information bits of $\mathbf{I}_1[k]$ at the rate of $C((\gamma_2/(\gamma_3+1))$ is given by

$$T_2 = \frac{|\mathbf{I}_1[k]| - T_1 C\left(\frac{\gamma_1}{\gamma_3+1}\right)}{C\left(\frac{\gamma_2}{\gamma_3+1}\right)}. \tag{26}$$

Meanwhile, during the UL session, User 2 transmits the information bits of $\mathbf{I}_2[k]$ at the fixed rate of $R_2(\lambda)$, unless the DL transmission has been completed. As mentioned earlier in Section IV-A, the associated time required by User 2 for completing this transmission is represented by N. Then, it can be shown that $T_1 + T_2 < N$, which implies that, in Case 2.3, the DL transmission will be terminated earlier than the UL transmission. Hence, the practical framework of Case 2.3 is similar to that illustrated in Fig. 4, with the slight difference that, in Case 2.3, the DL period relies on two steps. In the first step, the RN broadcasts $\mathbf{I}_3[k]$ at the rate of $C(\gamma_1/(\gamma_3+1))$ for a time of T_1, where the transmission of the information bits of $\mathbf{I}_2[k]$ is completed. Then, in the next step, the RN broadcasts $\mathbf{I}_3[k]$ at the rate of $C(\gamma_2/(\gamma_3+1))$ for a time of T_2, during which the entire DL transmission is completed.

Hence, similar to the scenario depicted for the residual period in Fig. 4, during the residual period of Case 2.3, User 1 and User 2 also have to update their UL transmission rates to the rate pair of $[R_1'(\lambda'), R_2'(\lambda')]$, as stipulated in (18). Therefore, similar to the additional condition discussed in Section IV-B2 and stipulated by (19) and (20), we also have to find the specific rate pair of $[R_1'(\lambda'), R_2'(\lambda')]$, which is capable of simultaneously satisfying (18) and $R_2(\lambda)/R_1(\lambda) = R_2'(\lambda')/R_1'(\lambda')$. In this case, we have $R_1(\lambda)/R_2(\lambda) \in (1, (C(\gamma_1/(\gamma_3+1))/C(\gamma_2/(\gamma_1+\gamma_3+1)))]$ and $R_1'(\lambda')/R_2'(\lambda') \in [(C(\gamma_1/(\gamma_2+1))/C(\gamma_2)), (C(\gamma_1)/C(\gamma_2/(\gamma_1+1)))]$. Then, it can be shown that $(1, (C(\gamma_1/(\gamma_3+1))/C(\gamma_2/(\gamma_1+\gamma_3+1)))] \subset [(C(\gamma_1/(\gamma_2+1))/C(\gamma_2)), (C(\gamma_1)/C(\gamma_2/(\gamma_1+1)))]$. Hence, an appropriate rate pair of $[R_1'(\lambda'),$ AQ7 AQ8

$R_2'(\lambda')]$ always exists, which confirms the correct operation of our information allocation scheme formulated in (23).

Based on the holistic analysis provided in Section IV-B3, the overall achievable error-free data rate of Case 2.3 is given by

$$R^{\text{BD-DF-FDN, Case 2.3}}(\lambda) = \frac{|\mathbf{I}_1[k]| + |\mathbf{I}_2[k]|}{T_1 + T_2 + \frac{|\mathbf{I}_1[k]|+|\mathbf{I}_2[k]|-(T_1+T_2)[R_1(\lambda)+R_2(\lambda)]}{C(\gamma_1+\gamma_2)}}. \quad (27)$$

Furthermore, it can be shown that $R^{\text{BD-DF-FDN, Case 2.3}}(\lambda)$ is a monotonically increasing function of $R_2(\lambda)$. Hence, if we assign to User 2 its maximum transmission rate for the period preceding the residual period, we arrive at the MAEFDR of Case 2.3, which may be formulated as

$$\begin{aligned} R_{\max}^{\text{BD-DF-FDN}} &= \lim_{\lambda\to\lambda_0} R^{\text{BD-DF-FDN, Case 2.3}}(\lambda) \\ &= \frac{C(\gamma_1+\gamma_2)C\left(\frac{\gamma_1}{\gamma_3+1}\right)}{C\left(\frac{\gamma_1}{\gamma_3+1}\right)+\frac{1}{2}\left[C(\gamma_1+\gamma_2)-C\left(\frac{\gamma_1+\gamma_2}{\gamma_3+1}\right)\right]}, \\ &\quad \text{if } \gamma_1 + \left(\frac{1}{\gamma_3+1}\right)\gamma_1^2 > \gamma_2 \geq \gamma_1 \cap \lambda \in (\lambda_0, 1]. \end{aligned} \quad (28)$$

Apparently, (28) is equivalent to (22). Then, it can be formally shown that the MAEFDR of our BD-DF-FDN obtained for Case 2.1 is always lower than that obtained for Case 2.2 or 2.3. Hence, we finally arrive at Theorem 4.1.

Theorem 4.1: The MAEFDR of BD-DF-FDN is given by

$$R_{\max}^{\text{BD-DF-FDN}} = \begin{cases} \frac{C\left(\frac{\gamma_1+\gamma_2}{\gamma_3+1}\right)C(\gamma_1)}{C(\gamma_1)+C\left(\frac{\gamma_2}{\gamma_1+\gamma_3+1}\right)-C\left(\frac{\gamma_1}{\gamma_3+1}\right)}, & \text{if } \gamma_2 \geq \gamma_1 + \left(\frac{1}{\gamma_3+1}\right)\gamma_1^2 \\ \frac{C(\gamma_1+\gamma_2)C\left(\frac{\gamma_1}{\gamma_3+1}\right)}{C\left(\frac{\gamma_1}{\gamma_3+1}\right)+\frac{1}{2}\left[C(\gamma_1+\gamma_2)-C\left(\frac{\gamma_1+\gamma_2}{\gamma_3+1}\right)\right]}, & \text{if } \gamma_1 + \left(\frac{1}{\gamma_3+1}\right)\gamma_1^2 > \gamma_2 \geq \gamma_1 \end{cases} \quad (29)$$

where $\gamma_i,\ i \in \{1,2,3\}$ is the relevant SNR defined in (3). Apparently, according to the analysis stated in Section IV, particularly to (29), depending on different channel conditions and transmit power levels, i.e., different relationships among γ_i, $i \in \{1,2,3\}$, the algebraic representation of MAEFDR of our BD-DF-FDN will be categorized into two different formulas.

V. Simulation Results

First, it is assumed that the distance between User 2 and User 1 is normalized to unity. Then, the distance between User 2 and the RN is denoted by D_2 and that between User 1 and the RN is denoted by D_1. Hence, we have $D_2 + D_1 = 1.0$. Then, each sum rate demonstrated in the following figures is an average over simulating 10^6 random fading channels.

We first investigate the effects of both the SI and the RN's geographic location on the MAEFDR of BD-DF-FDN. The relevant simulation results are displayed in Fig. 5, where the parameters employed can be found in Table I. Furthermore, to demonstrate the advantages of the proposed BD-DF-FDN, the performance of the FD-based direct transmission (FD-DT) regime, which is summarized in Table II, is also shown in Fig. 5 as a benchmark.

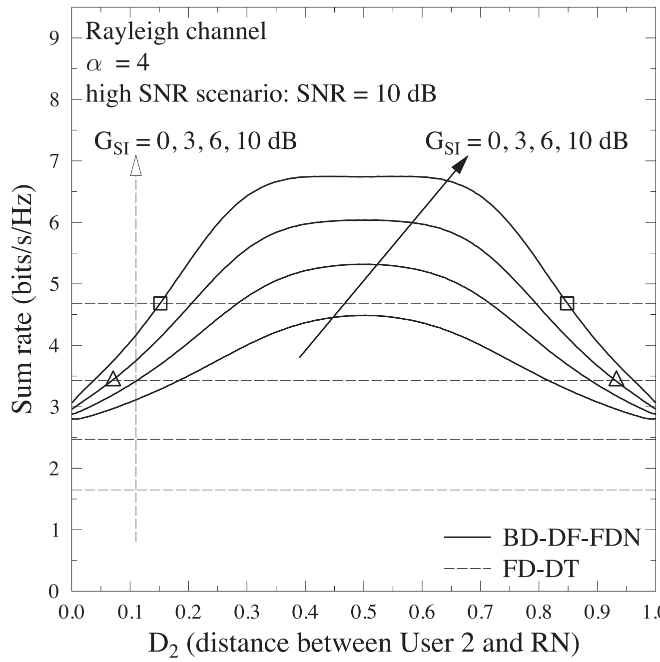

Fig. 5. Effects of both the SI and the RN's geographic location on the MAEFDR of BD-DF-FDN, which is evaluated according to (29) in Theorem 4.1.

TABLE I
System Parameters

Channel Model	Flat Block-Fading Channels
Number of Blocks	10^5
Path-Loss Exponent	$\alpha = 4$
SNR	$\frac{P}{\sigma^2} \in \{0,3,6,10\}$ dB
SI Suppression Factor	$G_{\text{SI}} \in \{0,3,6,10\}$ dB
Number of Positions	200

TABLE II
Competitive Networking Regimes

Regime	Description	Illustration
BD-DF-FDN	Two FD Users communicate with each other with the aid of FD-DF-TW relaying.	Fig. 1
BD-AF-FDN	Two FD Users communicate with each other with the aid of a full-duplex amplify-and-forward two-way relaying based RN.	[21, Fig. 1]
FD-DT	Two FD users communicate with each other using direct transmission (DT).	[20, Fig. 4]
DF-FDR relaying	Two HD users communicate with each other with the aid of a DF based full-duplex relay (DF-FDR).	[13, Fig. 1]
HD-DF-TW relaying	Two HD users communicate with each other with the aid of half-duplex DF two-way (HD-DF-TW) relaying.	[8, Fig. 1(b)]

It was reported in [19], [20] that contemporary FD transceiver techniques are capable of reducing the SI close to the noise floor. Hence, according to (2), it is achievable that $|\tilde{h}_3|^2 P \leq \sigma^2$, which is identical to $G_{\text{SI}} \geq \text{SNR}$. Hence, when the SNR value employed in Fig. 5 is 10 dB, it is reasonable to assume that we have $G_{\text{SI}} \in \{0,3,6,10\}$ dB for modeling

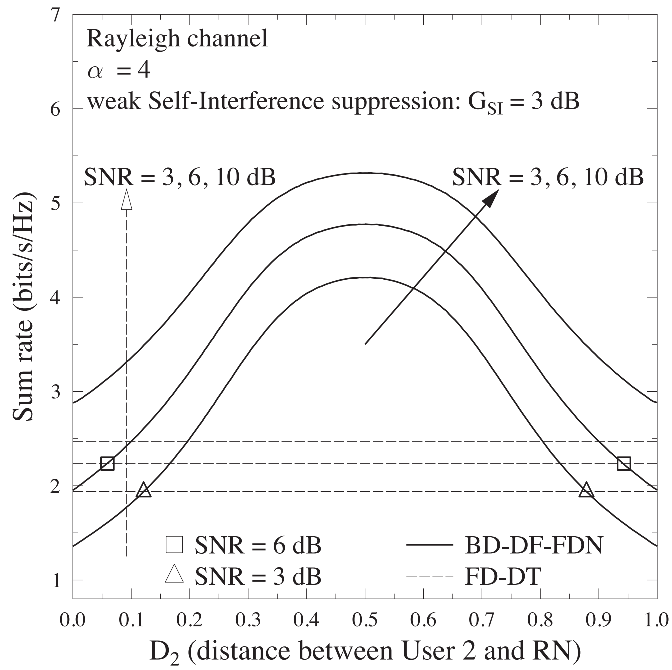

Fig. 6. Effect of the SNR value on the MAEFDR of BD-DF-FDN, which is evaluated according to (29) in Theorem 4.1. The parameters employed can be found in Table I.

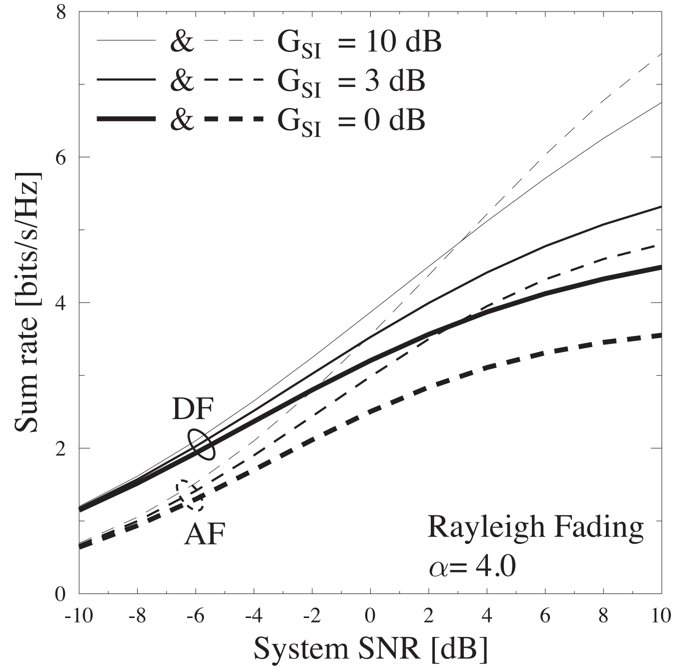

Fig. 7. Comparison between BD-DF-FDN and BD-AF-FDN in terms of their sum rate versus SNR performance, where their ability for resisting the impact of SI is highlighted.

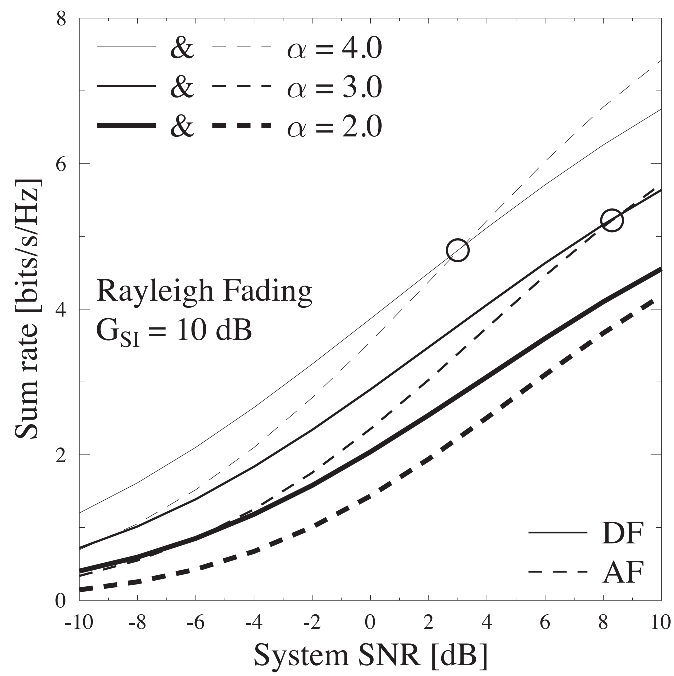

Fig. 8. Comparison between BD-DF-FDN and BD-AF-FDN. Different path-loss effects are investigated.

diverse scenarios, where we have a weak, mediocre, or powerful SI suppression capability.

As observed in Fig. 5, when we have $G_{\rm SI} = 0$ or 3 dB, the sum rate of our BD-DF-FDN always exceeds that of the FD-DT regime, regardless of the RN positions. However, when $G_{\rm SI}$ increases to 6 dB, the range of the RN's position, where our BD-DF-FDN outperforms the FD-DF regime, is reduced to the area between the two triangular legends shown in Fig. 5. More severely, when we have sufficiently high values of $G_{\rm SI} = 10$ dB, the predominant region of our BD-DF-FDN, with respect to its FD-DT counterpart, is further reduced to the area between the two square legends. Hence, it may be concluded from Fig. 5 that, for most practical SI suppression capabilities, our BD-DF-FDN has the potential of significantly improving the performance of an FD communication system. This is more suitable for FD-based communication scenarios, where the employment of powerful SI suppression cannot always be guaranteed.

Moreover, the MAEFDR of our BD-DF-FDN is also affected by the RN's position, as shown in Fig. 5. If the RN roams too close to one of the users, the system's sum rate will rapidly drop. This tendency can be evidenced again by comparing the sum rate of our BD-DF-FDN associated with $G_{\rm SI} = 10$ dB to that of the FD-DT regime, particularly when considering the curve segments between the two square legends in Fig. 5 in contrast to those outside these two square legends.

Similarly, in Fig. 6, we investigate the effect of different SNR values on the MAEFDR of BD-DF-FDN, when the SI suppression factor $G_{\rm SI}$ is fixed. Observe in Fig. 6 that, regardless of the SNR, the proposed BD-DF-FDN always outperforms its FD-DT regime-based counterpart, except when the RN is located too close to one of the users. Furthermore, the optimum performance is obtained in high-SNR scenarios.

Then, the comparisons between our BD-DF-FDN and the bidirectional AF-relaying-aided FD network (BD-AF-FDN) [21], which is also described in Table II, are demonstrated in Figs. 7 and 8. According to Figs. 7 and 8, in general, in contrast to its AF-based counterpart, the proposed BD-DF-FDN is capable of achieving a higher spectral efficiency during low-SNR regions. Specifically, when the SI suppression ability of the FD transceiver is enhanced to $G = 10$ dB,[7] the DF-aided

[7]It is equivalent to having $\Omega = 0.1$ in [21].

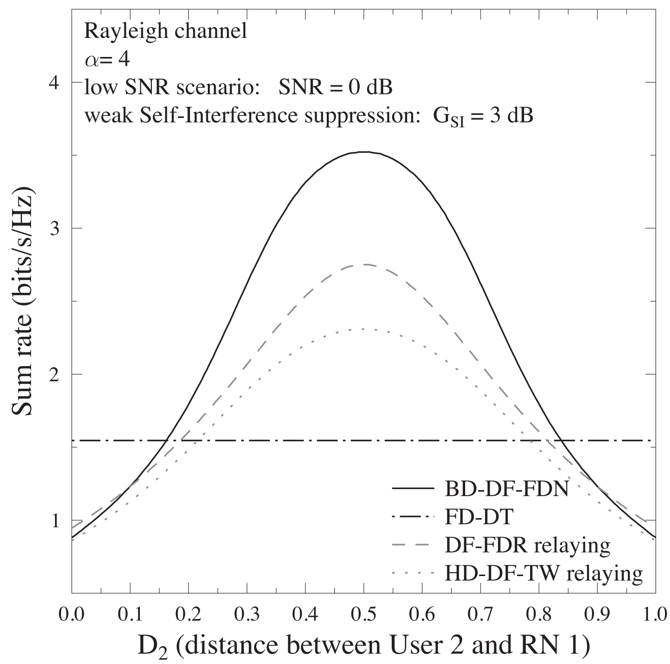

Fig. 9. Comparison among different regimes. The parameters employed can be found in Table I.

system can still outperform its AF-based counterpart within the low-SNR region of $(-\infty, 3]$ dB. Bearing the green radio concept in mind, with the aid of powerful forward error correction (FEC) techniques, in a mount of literatures, practical relaying systems tend to be operated in increasingly lower SNR scenarios [30]. Hence, the BD-DF-FDN may better adapt to the application scenarios, where powerful FEC receivers are employed.

In more detail, observe in Fig. 7 that the spectral gain of BD-DF-FDN, with respect to its AF-based counterpart, increases upon incurring higher SI. Then, observe in Fig. 8 that, when we fix the SI suppression ability of the FD transceiver, lower path-loss reduction effect will result in higher performance gain of the proposed DF-aided system compared with its AF-based counterpart. Based on these phenomena, it may be concluded that, in contrast to BD-AF-FDN [21], [22], our BD-DF-FDN seems to be more appropriate to low-SNR, high-SI, and low-PLRG application scenarios.

Finally, the spectral efficiency of our BD-DF-FDN regime versus that of other typical networking regimes is shown in Fig. 9, where the FDR-based system [10], [13] and the HD-DF-TW-based system [8] characterized in Table II are also invoked as benchmarks. Observe in Fig. 9 that, benefiting from the intelligent relaying strategy, the BD-DF-FDN is capable of significantly outperforming its DT-based counterpart, which also explores the advanced FD technology, except the situation that the RN roams extremely close to one of the users. Furthermore, the BD-DF-FDN is capable of achieving salient spectral gain, with regard to either the DF-FDR relaying or the HD-DF-TW relaying, which evidences the high spectral efficiency of combing a complete FD network with the intelligent two-way relaying strategy.

VI. Conclusion

In this paper, we have proposed the novel concept of bidirectional DF relaying. We considered a challenging FD communication scenario and conceived a bidirectional relaying-aided FD network, where an optimum rate allocation scheme was designed for improving the system's spectral efficiency.

The simulation results provided in Section V have confirmed that the proposed BD-DF-FDN is capable of achieving a significantly higher spectral efficiency than the other typical networking regimes listed in Table II. However, the performance of the BD-DF-FDN solution is dominated by the system's interference suppression capability, as well as by the RN's geographic location. Hence, in some scenarios where the system either has a weak or powerful interference suppression capability or if the RN is extremely close to one of the users, it may not be necessary to activate the proposed BD-DF-FDN.

References

[1] J. Y. Zhang, M. Matthaiou, G. K. Karagiannidis, Z. H. Tan, and H. B. Wang, "Gallager's exponent analysis of STBC MIMO systems over $\eta-\mu$ and $\kappa-\mu$ fading channels," *IEEE Trans. Commun.*, vol. 61, no. 3, pp. 1028–1039, Mar. 2013.

[2] J. N. Laneman, D. N. C. Tse, and G. W. Wornell, "Cooperative diversity in wireless networks: Efficient protocols and outage behavior," *IEEE Trans. Inf. Theory*, vol. 50, no. 12, pp. 3062–3080, Dec. 2004.

[3] A. Sendonaris, E. Erkip, and B. Aazhang, "User cooperation diversity—Part I: System description," *IEEE Trans. Commun.*, vol. 51, no. 11, pp. 1927–1938, Nov. 2003.

[4] G. Kramer, M. Gastpar, and P. Gupta, "Cooperative strategies and capacity theorems for relay networks," *IEEE Trans. Inf. Theory*, vol. 51, no. 9, pp. 3037–3063, Sep. 2005.

[5] B. Rankov and A. Wittneben, "Spectral efficient protocols for half-duplex fading relay channels," *IEEE J. Sel. Areas Commun.*, vol. 25, no. 2, pp. 379–389, Feb. 2007.

[6] L. Li, L. Wang, and L. Hanzo, "Successive AF/DF relaying in the cooperative DS-CDMA uplink: Capacity analysis and its system architecture," *IEEE Trans. Veh. Technol.*, vol. 62, no. 2, pp. 655–666, Feb. 2013.

[7] K. Jitvanichphaibool, R. Zhang, and Y. C. Liang, "Optimum resource allocation for two-way relay-assisted OFDMA," *IEEE Trans. Veh. Technol.*, vol. 58, no. 7, pp. 3311–3321, Sep. 2009.

[8] P. Popovski and H. Yomo, "Physical network coding in two-way wireless relay channels," in *Proc. IEEE ICC*, Jun. 2007, pp. 707–712.

[9] H. Ju, E. Oh, and D. Hong, "Catching resource-devouring worms in next-generation wireless relay systems: Two-way relay and full-duplex relay," *IEEE Commun. Mag.*, vol. 47, no. 9, pp. 58–65, Sep. 2009.

[10] H. Ju, E. Oh, and D. Hong, "Improving efficiency of resource usage in two-hop full duplex relay systems based on resource sharing and interference cancellation," *IEEE Trans. Wireless Commun.*, vol. 8, no. 8, pp. 3933–3938, Aug. 2009.

[11] T. Riihonen, S. Werner, and R. Wichman, "Mitigation of loopback self-interference in full-duplex MIMO relays," *IEEE Trans. Signal Process.*, vol. 59, no. 12, pp. 5983–5993, Dec. 2011.

[12] T. Kwon, S. Lim, S. Choi, and D. Hong, "Optimum duplex mode for DF relay in terms of the outage probability," *IEEE Trans. Veh. Technol.*, vol. 59, no. 7, pp. 3628–3634, Sep. 2010.

[13] T. Riihonen, S. Werner, and R. Wichman, "Hybrid full-duplex/half-duplex relaying with transmit power adaptation," *IEEE Trans. Wireless Commun.*, vol. 10, no. 9, pp. 3074–3085, Sep. 2011.

[14] B. P. Day, A. R. Margetts, D. B. Bliss, and P. Schniter, "Full-duplex MIMO relaying: Achievable rate under limited dynamic region," *IEEE J. Sel. Areas Commun.*, vol. 30, no. 8, pp. 1541–1553, Sep. 2012.

[15] H. Ju, S. Lim, D. Kim, H. V. Poor, and D. Hong, "Full duplexity in beamforming-based multi-hop relay networks," *IEEE J. Sel. Areas Commun.*, vol. 30, no. 8, pp. 1554–1564, Sep. 2012.

[16] T. K. Baranwal, D. S. Michalopoulos, and R. Schober, "Outage analysis of multihop full duplex relaying," *IEEE Commun. Lett.*, vol. 17, no. 1, pp. 63–66, Jan. 2013.

[17] J. I. Choi, M. Jain, K. Srinivasan, P. Levis, and S. Katti, "Achieving single channel, full duplex wireless communication," in *Proc. 16th Annu. Int. Conf. Mobile Comput. Netw.*, 2010, pp. 1–12.

[18] M. Jain *et al.*, "Practical, real-time, full duplex wireless," in *Proc. 17th Annu. Int. Conf. Mobile Comput. Netw.*, 2011, pp. 301–312.

[19] D. Bharadia, E. McMilin, and S. Katti, "Full duplex radios," in *Proc. ACM SIGCOMM*, 2013, pp. 375–386.

[20] S. Hong *et al.*, "Application of self-interference cancellation in 5G and beyond," *IEEE Commun. Mag.*, vol. 52, no. 2, pp. 114–121, Feb. 2014.

[21] X. Cheng, B. Yu, X. Cheng, and L. Yang, "Two-way full-duplex amplify-and-forward relaying," in *Proc. IEEE Mil. Commun. Conf.*, Nov. 2013, pp. 1–6.

[22] H. Cui, M. Ma, L. Song, and B. Jiao, "Relay selection for two-way full duplex relay networks with amplify-and-forward protocol," *IEEE Trans. Wireless Commun.*, vol. 13, no. 7, pp. 3768–3777, Jul. 2014.

[23] G. Zheng, "Joint beamforming optimization and power control for full-duplex MIMO two-way relay channel," *IEEE Trans. Signal Process.*, vol. 63, no. 3, pp. 555–566, Feb. 2015.

[24] R. Ahlswede, N. Cai, S.-Y. R. Li, and R. W. Yeung, "Network information flow," *IEEE Trans. Inf. Theory*, vol. 46, no. 4, pp. 1204–1216, Jul. 2000.

[25] R. Koetter and M. Medard, "An algebraic approach to network coding," *IEEE/ACM Trans. Netw.*, vol. 11, no. 5, pp. 782–795, Oct. 2003.

[26] L. Xiao, T. Fuja, J. Kliewer, and D. Costello, "A network coding approach to cooperative diversity," *IEEE Trans. Inf. Theory*, vol. 53, no. 10, pp. 3714–3722, Oct. 2007.

[27] L. Li, L. Wang, and L. Hanzo, "Generalized adaptive network coding aided successive relaying for noncoherent cooperation," *IEEE Trans. Commun.*, vol. 61, no. 5, pp. 1750–1763, May 2013.

[28] T. S. Rappaport, *Wireless Communications: Principles and Practice*. Upper Saddle River, NJ, USA: Prentice-Hall, 2002.

[29] T. M. Cover and J. A. Thomas, *Elements of Information Theory*. Hoboken, NJ, USA: Wiley, 2006.

[30] L. Hanzo, O. R. Alamri, M. El-Hajjar and N. Wu, *Near-Capacity Multi-Functional MIMO Systems: Sphere-Packing, Iterative Detection and Cooperation*. Hoboken, NJ, USA: Wiley, May 2009.

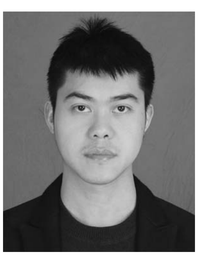

Li Li received the Ph.D. degree in electronics and computer science, in October 2013, from the University of Southampton, Southampton, U.K., working with the Southampton Wireless (SW) Group.

Upon completion of his Ph.D. studies, he conducted research as a Senior Research Assistant with the School of Electronics and Computer Science, University of Southampton, from December 2013 to December 2014, where he participated in the European Union Concerto Project. In January 2015, he joined the Provincial Key Laboratory of Information Coding and Transmission, Southwest Jiaotong University, Chengdu, China, serving as a Lecturer. His research interests include channel coding, iterative detection, noncoherent transmission technologies, cooperative communications, network coding, and nonorthogonal multiple-access techniques.

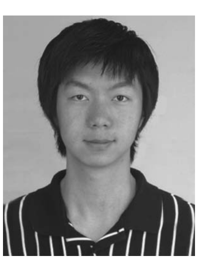

Chen Dong received the B.S. degree in electronic information sciences and technology from the University of Science and Technology of China, Hefei, China, in 2004; the M.Eng. degree in pattern recognition and automation from the Chinese Academy of Sciences, Beijing, China, in 2007; and the Ph.D. degree from the University of Southampton, Southampton, U.K., in 2014.

Following his Ph.D. studies, was a Postdoctoral Researcher with the University of Southampton for one year. In 2015, he joined the R&D Center AQ9 of Huawei Technologies, Shenzhen, China. His research interests include applied mathematics, relaying systems, channel modeling, and cross-layer optimization.

Dr. Dong received a scholarship under the UK-China Scholarships for Excellence Programme and the Best Paper Award at the 2014 IEEE Vehicular Technology Conference (VTC Fall).

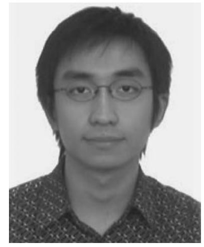

Li Wang (S'09–M'10) was born in Chengdu, China, in 1982. He received the B.Eng. degree in information engineering from the Chengdu University of Technology in 2005 and the M.Sc. degree with distinction in radio frequency communication systems and the Ph.D. degree in electronics and computer science from the University of Southampton, Southampton, U.K., in 2006 and 2010, respectively.

Between October 2006 and January 2010, he participated in the Delivery Efficiency Core Research Programme of the Virtual Centre of Excellence in Mobile and Personal Communications (Mobile VCE). Upon completion of his Ph.D. studies in January 2010, he was a Senior Research Fellow with the School of Electronics and Computer Science, University of Southampton. During this period, he was involved in projects for the India-UK Advanced Technology Centre. In March 2012, he joined the R&D Center of Huawei Technologies, Stockholm, Sweden, where he is currently a Algorithm Specialist in both the radio transmission technology and radio resource management areas. He has published 35 research papers in IEEE/IET journals and conferences, and he has coauthored one John Wiley/IEEE Press book. He has broad research interests in the field of wireless communications, including physical (PHY) layer modeling, link adaptation, cross-layer system design, multicarrier transmission, multi-input–multi-output (MIMO) techniques, coordinated multipoint (CoMP) AQ10 transmission, channel coding, multiuser detection, noncoherent transmission techniques, advanced iterative receiver design, and adaptive filters. He is now conducting pioneering cross-discipline researches to build next-generation communication systems with artificial intelligence.

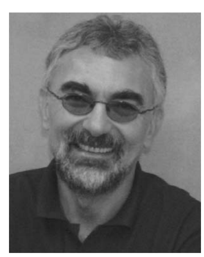

Lajos Hanzo (M'91–SM'92–F'04) received the M.S. degree in electronics and the Ph.D. degree from the Technical University of Budapest (currently the Budapest University of Technology and Economics), Budapest, Hungary, in 1976 and 1983, respectively; the D.Sc. degree from the Southampton University, Southampton, U.K., in 2004; and the "Doctor Honoris Causa" degree from the Budapest University of Technology and Economics in 2009.

During his 35-year career in telecommunications, he has held various research and academic posts in Hungary, Germany, and the U.K. Since 1986, he has been with the School of Electronics and Computer Science, University of Southampton, where he holds the Chair in Telecommunications. He is currently directing a 100-strong academic research team, working on a range of research projects in the field of wireless multimedia communications sponsored by industry, the Engineering and Physical Sciences Research Council of the U.K., the European IST Programme, and the Mobile Virtual Centre of Excellence (VCE), U.K. During 2008–2012, he was a Chaired Professor with Tsinghua University, Beijing, China. He is an enthusiastic supporter of industrial and academic liaison and offers a range of industrial courses. He has successfully supervised more than 80 Ph.D. students, coauthored 20 John Wiley/IEEE Press books on mobile radio communications, totaling in excess of 10 000 pages, and published more than 1500 research entries on IEEE Xplore. His research is funded by the European Research Council's Senior Research Fellow Grant.

Dr. Hanzo is a Fellow of the Royal Academy of Engineering, The Institution of Engineering and Technology, and the European Association for Signal Processing. He is also a Governor of the IEEE Vehicular Technology Society. During 2008–2012, he was the Editor-in-Chief of the IEEE Press. He has served as the Technical Program Committee and General Chair of IEEE conferences, has presented keynote lectures, and has received number of distinctions. For further information on research in progress and associated publications see http://www-mobile.ecs.soton.ac.uk

AUTHOR QUERIES

AUTHOR PLEASE ANSWER ALL QUERIES

AQ1 = Please provide keywords.
AQ2 = Please check if the expanded form of RC is properly captured; otherwise, kindly provide the correction.
AQ3 = Please check if changes in this sentence are properly captured, to make the statement clear; otherwise, kindly provide the correction.
AQ4 = Please check if $|\mathbf{I}_2[k]|, |\mathbf{I}_2[k]|$ here should be changed to $|\mathbf{I}_1[k]|, |\mathbf{I}_2[k]|$, to avoid redundancy; otherwise kindly provide the correction.
AQ5 = Please check if $\mathbf{I}_1[k]$ and $\mathbf{I}_1[k]$ here should be changed to $\mathbf{I}_1[k]$ and $\mathbf{I}_2[k]$, to avoid redundancy; otherwise, kindly provide the correction.
AQ6 = Please check if you wish to capture the equations in this sentence as displayed equations; otherwise, kindly provide the correction.
AQ7 = Please check if you wish to capture the equations in this sentence as displayed equations; otherwise, kindly provide the correction.
AQ8 = Please check if you wish to capture the equations in this sentence as displayed equations; otherwise, kindly provide the correction.
AQ9 = Please check if the city location "Shenzhen" is properly captured here, to match the current affiliation of author C. Dong in the affiliation footnote; otherwise, kindly provide the correction.
AQ10 = Please check if the expanded form of CoMP is properly captured; otherwise, kindly provide the correction.

END OF ALL QUERIES